Soft Matter

View Online
Dynamic Article Links

Cite this: *Soft Matter*, 2011, **7**, 4964

www.rsc.org/softmatter

PAPER

Spider silk-bone sialoprotein fusion proteins for bone tissue engineering†

Sílvia Gomes,[abc] Isabel B. Leonor,[ab] João F. Mano,[ab] Rui L. Reis*[ab] and David L. Kaplan*[c]

Received 9th January 2011, Accepted 14th March 2011
DOI: 10.1039/c1sm05024a

The remarkable mechanical characteristics of the spider silk protein major ampullate spidroin protein suggest this polymer as a promising biomaterial to consider for the fabrication of scaffolds for bone regeneration. Herein, a new functionalized spider silk-bone sialoprotein fusion protein was designed, cloned, expressed, purified and the osteogenic activity studied. Bone sialoprotein (BSP) is a multi-domain protein with the ability to induce cell attachment and differentiation and the deposition of calcium phosphates (CaP). Attenuated Total Reflection Fourier Transform Infrared (ATR-FTIR) was used to assess the secondary structure of the fusion protein. *In vitro* mineralization studies demonstrated that this new fusion protein with BSP retained the ability to induce the deposition of CaP. Studies *in vitro* indicated that human mesenchymal stem cells had significant improvement towards osteogenic outcomes when cultivated in the presence of the new fusion protein *vs.* silk alone. The present work demonstrates the potential of this new fusion protein for future applications in bone regeneration.

1. Introduction

The increasing demand for organs and tissues to replace damaged or diseased systems represents a major health challenge worldwide. Bone grafting is the second most frequent transplant procedure after blood transfusion. Transplantation of bone tissue from autogeneic and allogeneic sources has been a major strategy in tissue repair. However, major challenges regarding transplantation remain, including the limited availability of suitable and safe tissues and organs, frequent adverse immune responses and disease transmission, loss of biological and mechanical properties after processing, high costs and worldwide scarcity.[1] As an option, tissue engineering has been explored for bone regeneration with the objective of generating bone functional equivalents to overcome the limitations of the currently used methodologies mentioned above.[2] For this purpose different polymers with diverse mechanical and biological characteristics have been studied with respect to support for regeneration of damaged bone tissue.[3–5]

Silk proteins, derived from spiders and silkworms, are particularly relevant polymers for consideration as biomaterial scaffolds for bone regeneration. Silks harbour remarkable mechanical properties, while also offering slow biodegradation *in vivo* and appropriate biological compatibility.[6] While silkworm silk has been extensively studied with regard to bone tissue formation *in vitro* and *in vivo*, spider silks have been less studied in this context.

Spiders produce different types of silk for different functions. Among these different silk types, the major ampullate silk, or dragline silk, secreted by the major ampullate gland presents tensile strength comparable to Kevlar (4×10^9 N m^{-2}) and extensibility around 35%, compared to 5% for Kevlar.[7] Major ampullate silk protein has a molecular structure comprising β-sheet forming crystalline regions that alternate with less organized regions. These two regions correspond to two chemically distinct blocks in the protein polymer chains, where the hydrophilic GGX motifs (G stands for glycine and X is mostly glutamine) are responsible for the less crystalline regions and the poly-alanine (poly-A) motifs form the crystalline regions. The hydrophobic poly-A motifs are responsible for the formation of rigid and highly packed anti-parallel β-sheets[8] due to hydrogen bonding, generating the physical cross-links that stabilize silk structures in these crystalline regions. The GGX motif adopts a helical conformation forming amorphous regions that connect the poly-A motifs providing elasticity to the silk fibers.[9] The combination of glycine-rich domains with the poly-A regions and the formation of β-sheet cross-links between blocks give rise to the impressive mechanical properties of major ampullate silk fibers.[10]

The silk from the silkworm *Bombyx mori* can be supplied in large scale by sericulture, however, no equivalent production

[a]*3B's Research Group—Biomaterials, Biodegradables and Biomimetics, Department of Polymer Engineering, University of Minho, Headquarters of the European Institute of Excellence on Tissue Engineering and Regenerative Medicine, AvePark, Taipas, Guimarães, Portugal. E-mail: rgreis@dep.uminho.pt; Fax: +351 253 510 909; Tel: +351 253 510 900*
[b]*IBB-Institute for Biotechnology and Bioengineering, PT Associated Laboratory, Guimarães, Portugal. Fax: +351 253 510 909; Tel: +351 253 510 900*
[c]*Departments of Biomedical Engineering, Chemistry and Physics, Tufts University, Medford, Massachusetts, 02155, USA. E-mail: David.Kaplan@tufts.edu; Fax: +16176272580; Tel: +16176273231*
† Electronic supplementary information (ESI) available. See DOI: 10.1039/c1sm05024a

process is currently available for spider silks. For this reason the production of spider silk is carried out in heterologous expression systems, such as *Escherichia coli*, as used by us and other research groups to provide sufficient spider silk for study.[10,11] Furthermore, the use of recombinant DNA technology in the synthesis of these protein-based biopolymers has significant advantages over conventional production systems, allowing precise control of the protein primary sequence and thus its chemistry, and control of block distribution.[11] The major ampullate spidroin protein (MaSpI), produced by the spider species *Nephila clavipes*, is one of the spider silks most extensively studied using recombinant DNA technology.[7] Compared with *Bombyx mori* silk spider silk is stronger and has no immunogenic coat of sericin as in the case of *B. mori* silk.[12] Furthermore, the high strength, toughness and light weight properties of spider silk, along with expression in heterologous systems make MaSpI a suitable choice for the fabrication of high performance biomaterials for bone regeneration applications.

An advantage of using genetically engineered fibrous proteins such as spider silks is the possibility of generating new genetic variants carrying new functional domains. Therefore the synthesis of new chimeric proteins with enhanced features when compared with the native isolated counterparts can offer multifunctional features that otherwise are difficult to obtain, require extensive chemical modifications or are challenging to control during preparation. Thus, MaSpI can be expressed together with other proteins resulting in new chimeric proteins, retaining the self-assembly and outstanding mechanical performance of the native silk materials, but adding new functional features to improve or control biocompatibility and osseointegration. We have previously demonstrated this approach with both silica[13] and hydroxyapatite[14] nucleation domains fused to spider silk.

The ability of bone sialoprotein (BSP) to induce the attachment and migration of endothelial cells,[15] together with adhesion and differentiation of osteoblasts[16] related to bone remodelling has been demonstrated.[17] The ability to induce cell adhesion is related to the presence of a C-terminal RGD sequence in BSP that binds to integrins.[18–22] Additionally, *in vivo* studies indicate that incorporation of BSP into collagen[23,24] or titanium[25] implants promoted osteoblast differentiation and proliferation and enhanced osteoinductive effects. Furthermore, BSP is also responsible for the deposition of calcium phosphate in bone tissues, especially after association with collagen type I.[26] There is some evidence that in the early stages of mineralization hydroxyapatite crystals nucleate and grow inside the 68 nm gaps (hole zones) present between the triple-helical collagen fibrils. The labelling of BSP allowed the detection of the protein in these hole zones between the collagen fibrils suggesting that this protein may regulate the onset of calcification.[27] Additionally, different studies address the ability of BSP protein to interact with different binding partners[28] including collagen,[26] hydroxyapatite,[29] matrix metalloproteinase, factor H,[30] and integrin $\alpha_v\beta_3$ present in cell membranes[18,19]

The objective of the present study was the generation of a new silk fusion protein through the combination of BSP and MaSp1 consensus sequences. The silk block carries six repeats of the consensus repeat unit for the native sequence of the major ampullate dragline silk I from *N. clavipes*. Each silk repeat is formed by a hydrophilic GGX motif and a hydrophobic poly-A motif.

The present work describes the assembly of a new molecular-level biomaterial combining a spider silk consensus sequence with the complete sequence for BSP. When compared with previous silk chimeras[13,14] this new fusion protein has the advantage of combining the remarkable mechanical performance and self-assembly capability of silk with the multi-domain BSP sequence. This multi-domain BSP is advantageous for the concurrent control of the different processes related to osteogenesis described above.

2. Results and discussion

The presence of the BSP insert in the cloning vector containing the silk modules was confirmed through DNA sequencing. SDS-PAGE indicated that both expression and purification of the 6mer + BSP and the silk control, only 6mer, were successful and protein sequencing confirmed the *N*-terminal amino acid sequence. The purity level for both proteins was around 95% for 6mer and 90% for 6mer + BSP. For 6mer + BSP protein the theoretical molecular weight is approximately 52 kDa and with SDS-PAGE it was possible to observe a strong band at around 49 kDa. In the case of the 6mer the estimated molecular weight is approximately 21.8 kDa and the SDS-PAGE showed a band at 28 kDa (Fig. 1). This discrepancy between the expected and observed molecular weight in the case of 6mer protein has been reported previously for other silk proteins.[31–33] During SDS-PAGE the migration rate of proteins can be affected not only by its size but also by the protein shape.[34] The tendency of silk proteins to aggregate can be a possible cause for their slow migration during electrophoresis. After purification, dialysis and lyophilization the yields of 6mer + BSP and 6mer were approximately 17 mg L^{-1} and 25 mg L^{-1}, respectively.

The expressed 6mer + BSP and 6mer proteins were used to cast 2% protein films that were self-supporting after dehydration and methanol treatment. ATR-FTIR analysis to the 6mer + BSP protein films demonstrated that the introduction of the BSP domain with the spider silk did not disrupt the self-assembly capacity of the silk sequence, manifested through the formation

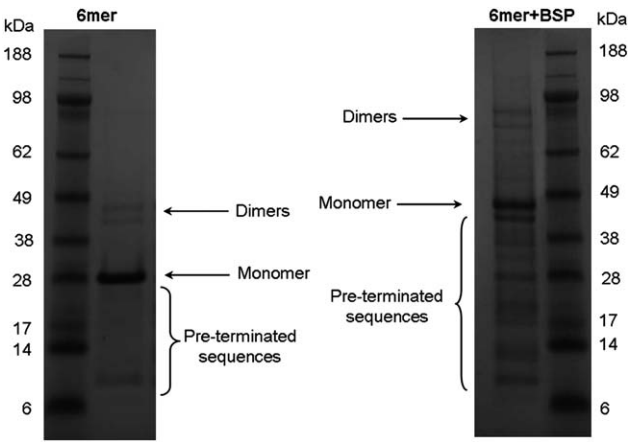

Fig. 1 SDS-PAGE gels for 6mer and 6mer + BSP proteins, stained with colloidal blue.

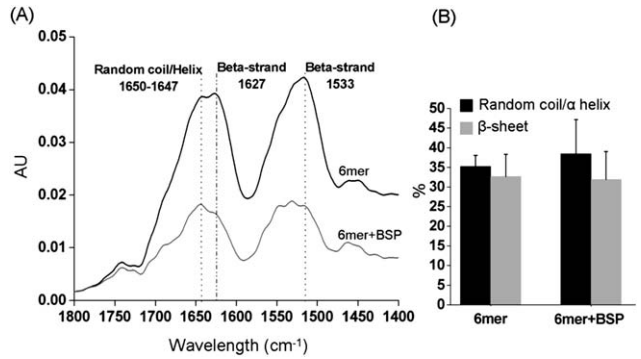

Fig. 2 (A) ATR-FTIR spectra of the 6mer and 6mer + BSP films after 2 hours treatment with 70% methanol. (B) Percentage of β-sheet and random coil/helix conformations after ATR-FTIR spectra deconvolution of the 6mer and 6mer + BSP films.

of β-sheet after treatment with methanol (Fig. 2). The ATR-FTIR spectra of 6mer and 6mer + BSP films after 2 hours treatment with 70% methanol solution exhibited strong amide I (1700–1600 cm^{-1}) and amide II (1600–1500 cm^{-1}) regions (Fig. 2A). ATR-FTIR spectra for both protein films, 6mer + BSP and 6mer, exhibited vibrational modes in the range of 1650–1647 cm^{-1} amide I region, indicative of helix/random coil conformations and in the range of 1626–1628 cm^{-1}, amide I region, and at 1533 cm^{-1}, amide II region, both peaks indicative of antiparallel β-sheet structures.[35–37] After spectral deconvolution the percentage of helix/random coil and antiparallel β-sheet structures was determined (Fig. 2B). For both protein films the percentage of secondary structures was similar and statistical analysis indicated no significant differences ($p > 0.05$) between the 6mer + BSP and 6mer control films. For helix/random coil conformations the percentages were 35% for the 6mer films and 37% for the 6mer + BSP films. For β-sheet structures the percentages were 33% and 32% for the 6mer and 6mer + BSP films, respectively.

Furthermore, this new protein retained the function of BSP to induce the nucleation of calcium phosphate (CaP), confirmed by energy dispersive spectroscopy (EDS) and field-emission scanning electron microscopy (SEM). After 1 hour in accelerated calcification solution (ACS) at 37 °C SEM analysis did not generate evidence for the formation of minerals on either film, 6mer or 6mer + BSP (Fig. 3A). However, EDS analysis indicated the presence of calcium (Ca) and phosphorus (P) in the 6mer + BSP films but not in the 6mer films (Fig. 3B). The Ca/P ratios in 6mer + BSP films varied between 1.72 and 1.86. After 6 hours of incubation it was possible to observe by SEM the formation of mineral aggregates on the surface of the 6mer + BSP films, with diameters around 8–10 μm (Fig. 3A). EDS analysis indicated a composition for Ca and P with Ca/P ratios between 1.82 and 2.03 (Fig. 3B). At longer timescales mineral deposition continues (data not shown). These results indicate the ability of the 6mer + BSP sequence to induce the nucleation of CaP, due to the presence of the BSP domain, a sequence known to be involved in the mineralization process in bone tissue.[27,29] For the 6mer films, the formation of mineral was not observed even after 6 hours (Fig. 3A). These results are in agreement with the EDS analysis, where no mineral was detected on the 6mer control films surface after 6 hours of immersion in ACS (Fig. 3B).

After 3 days in osteogenic culture media no mineral formation was observed on the surface of the 6mer + BSP films (Fig. 4), although EDS characterization confirmed the presence of Ca on the surface (Fig. 5). Ca/P ratios were 0 after 3 days of culture for

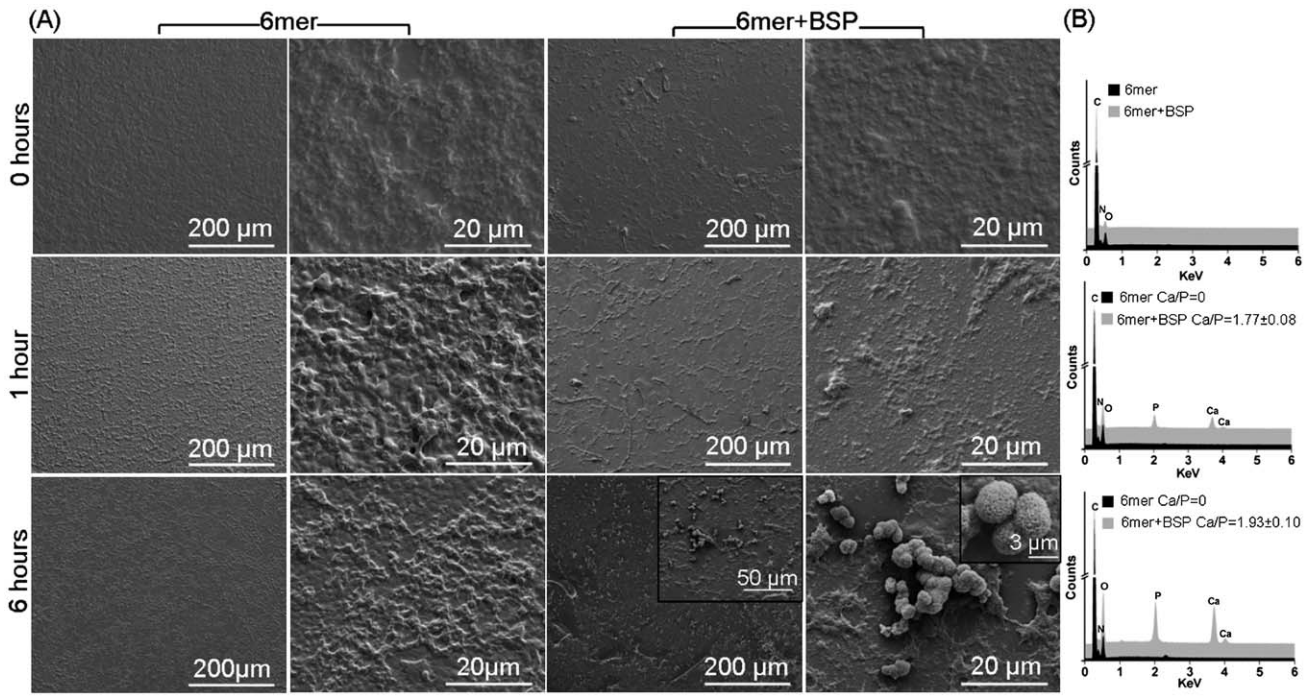

Fig. 3 (A) Surface morphologies and (B) EDS characterization of the 6mer and 6mer + BSP films before and after soaking in ACS solution for 1 and 6 hours.

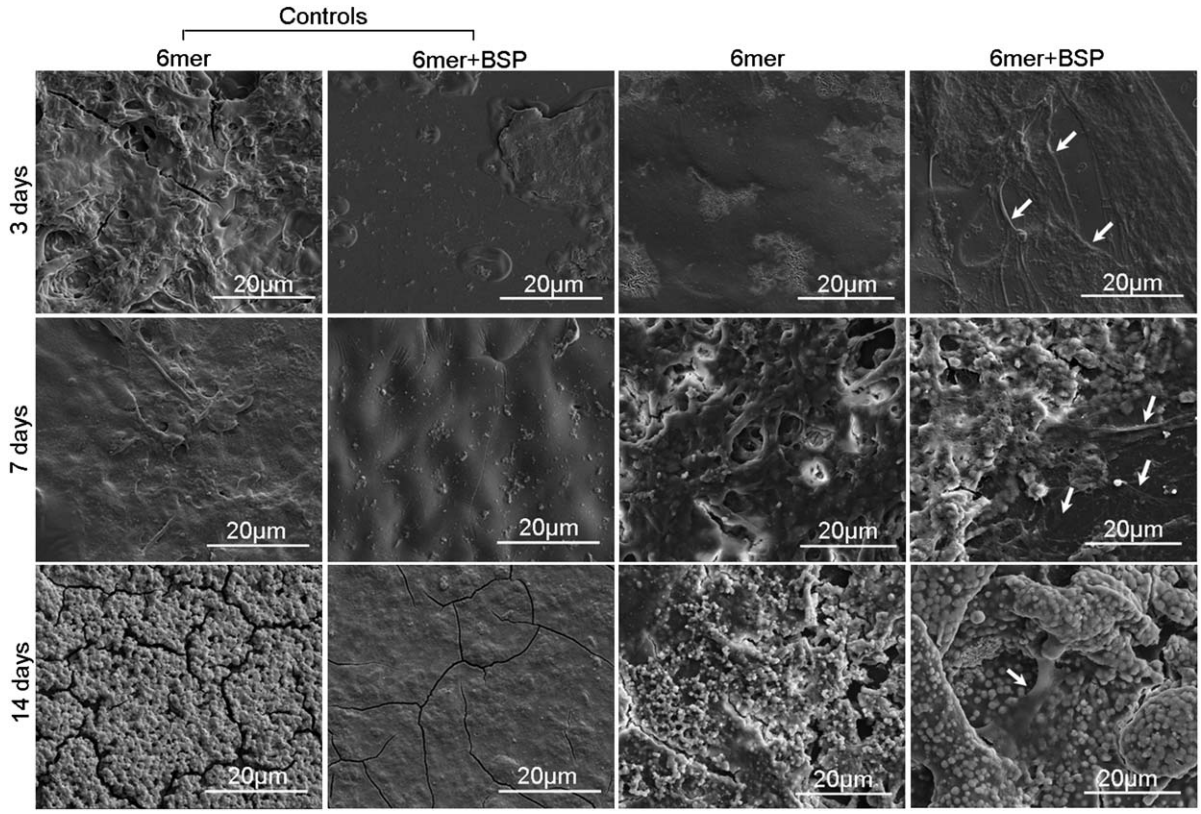

Fig. 4 Morphology of the 6mer and 6mer + BSP films seeded with hMSCs and cultured for 3, 7 and 14 days. In all assays, the 6mer and 6mer + BSP films without cells were used as controls. White arrows mark cells with osteoblast-like morphology.

6mer and 6mer + BSP films and for the controls with no cells, therefore these values were excluded from Fig. 5.

EDS characterization of 6mer + BSP samples after 7 and 14 days of cell culture in osteogenic culture medium indicated an significant increase ($p = 0.005$) in Ca/P ratios from 0.90–1.19 at day 7 to values between 1.53 and 1.72 at day 14 (Fig. 5). These last values are very close to those found for tricalcium phosphate (1.50) and hydroxyapatite (1.67), respectively.[38] For 6mer samples there was also a slight increase in the Ca/P ratio between day 7 and day 14, from 0.58–0.90 to 0.64–0.93, respectively, however with no statistical significance. Additionally, statistical comparison indicated that the Ca/P ratio in 6mer films after 14 days of culture was significantly lower ($p = 0.003$) than the Ca/P ratio in 6mer + BSP films (Fig. 5).

EDS analyses for the controls, 6mer + BSP and 6mer films incubated in osteogenic medium without cells, indicated the precipitation of CaP in both types of films after 7 and 14 days of culture. In the case of 6mer + BSP controls the calcium content is around 1.9 and 1.7 (ESI†) after 3 and 7 days of incubation in osteogenic medium, respectively, with Ca/P ratios as high as 7.16 after 7 days. In the case of 6mer controls the calcium content is around 0.3 after 3 and 7 days (ESI†). A possible explanation for this can be the affinity of the BSP domain in the 6mer + BSP protein to bind calcium ions. When the time of culture is increased to 14 days this effect is superimposed by the continuous precipitation of calcium and phosphate and the Ca/P ratios for 6mer + BSP and 6mer controls reach similar values. Furthermore, for 6mer films without cells, after 7 days of culture, the Ca/P ratio was significantly higher than the ratio registered for these samples when incubated in the presence of cells. This fact was also noted for the 6mer + BSP films without cells that registered, after 7 days of culture, Ca/P ratios between 0 and 7.16 *versus* 0.89 and 1.18 for 6mer + BSP films with cells. However, statistical analysis showed no significant difference between both conditions. After 14 days of culture, Ca/P ratios reached values between 1.26 and 2.07 for 6mer + BSP films without cells, *versus* 1.53–1.72 obtained for 6mer + BSP films with cells (Fig. 5). This extended range of Ca/P ratios for 6mer + BSP controls leads to higher standard deviations when compared with 6mer + BSP films with cells (Fig. 5) and could be caused by uncontrolled mineralization processes taking place in 6mer + BSP controls without cells.

SEM characterization provided an assessment of the morphology of the CaP formed on the films after cell culture. The morphologies of the minerals were different, mainly in the case of the 6mer + BSP films after cell culture *vs.* 6mer + BSP films incubated with no cells (control) (Fig. 4). At day 14 the CaP films formed on 6mer + BSP films presented a globular cauliflower-like morphology while for the control samples, 6mer + BSP films without cells, a flat layer of CaP was observed (Fig. 4). Both the SEM and EDS results suggest that these differences in mineral morphology and in Ca/P deposition may be the result from the presence of cells that might play a role in the deposition and modulation of calcium phosphates, inducing a more controlled mineralization process. SEM characterization also found that the human mesenchymal stem cells (hMSC) cultivated on

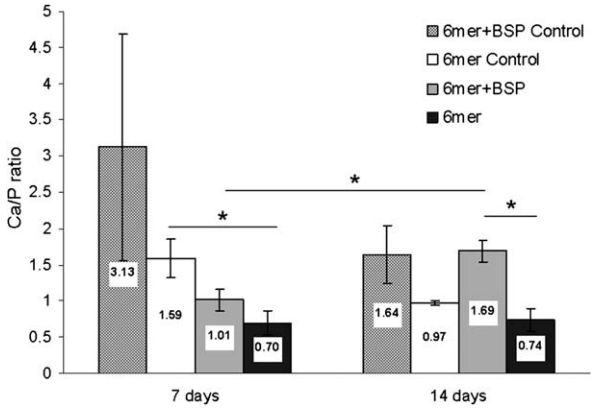

Fig. 5 Ca/P ratios determined by EDS after 7 and 14 days of culture with cells, 6mer and 6mer + BSP, and without cells, 6mer and 6mer + BSP controls. The values in each bar correspond to the average Ca/P ratio. Asterisks indicate statistically significant differences ($p < 0.05$).

6mer + BSP films during the 3, 7 and 14 days of culture in osteogenic differentiation medium had osteoblastic-like morphology, based on their flattened and polygonal morphology with multiple filopodia or very thin extensions[39] (Fig. 4). Cell viability/proliferation was measured after 3, 7 and 14 days of culture in osteogenic medium using the Alamar Blue assay.

Results indicated that hMSCs cultured on 6mer + BSP films supported higher cell viability/proliferation ($p < 0.05$) than cells cultured on 6mer films (Fig. 6).

The presence of cell binding domains in the 6mer + BSP protein within the BSP sequence,[15,16] may be responsible for the cell response when compared with control samples. Several studies describe the incorporation of RGD sequences to enhance cell responses to biomaterials.[40,41] The coupling of the RGD triplet to different silk matrices significantly increased the adhesion and proliferation of different cell types such as bone marrow stromal cells,[42] human corneal fibroblasts[43] and osteoblasts like cells (Saos-2). Also, in some studies transcript levels of collagen I[42] and osteocalcin[44] increased significantly when Saos-2 and

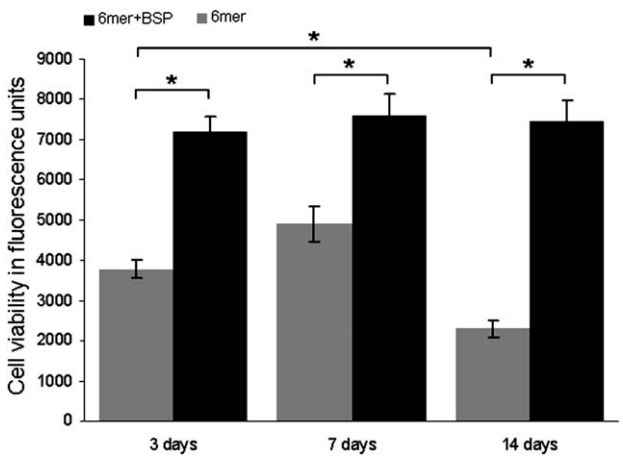

Fig. 6 Viability of cells seeded on the 6mer and 6mer + BSP films for 3, 7 and 14 days of culture and determined by Alamar Blue. Cell viability is expressed in relative fluorescence units. Asterisks indicate statistically significant differences ($p < 0.05$).

human corneal fibroblasts were cultivated in silk matrices functionalized with RGD. Furthermore, calcification was also significantly elevated in the presence of RGD sequences.[44] So, in the present study the presence of the RGD triplet in the BSP sequence of 6mer + BSP protein enhanced cell responses which can potentiate the production of mineralized extracellular matrix. However this effect can overlap with the potential of the BSP epitopes to induce CaP nucleation.

For the 6mer films, osteoblast-like morphology was not as evident and a reduction in viability/proliferation was observed after 3, 7 and 14 days in osteogenic medium.

Quantitative real time reverse transcription-polymerase chain reaction (quantitative real time RT-PCR) was used to assess the expression of alkaline phosphatase (ALP), integrin bone sialoprotein (IBSP), collagen type I α 1 (COL1A1) and collagen type II α 1 (COL2A1). The expression of bone-related genes by hMSCs cultured on 6mer + BSP indicated significant ($p < 0.05$) up-regulation of ALP, IBSP and COL1A1 during 14 days of cell culture (Fig. 7). For the 6mer samples a significant decrease ($p < 0.05$) in the expression level was observed for ALP, COL1A1 from day 3 to day 14, and the expression of IBSP gene was low at days 3 and 7 and increased at day 14 (Fig.7).

ALP transcript levels for both 6mer + BSP and 6mer films were similar for days 3 and 7, while day 14 transcript levels were significantly ($p < 0.05$) higher on the 6mer + BSP samples. ALP is considered an osteoblast marker[45] and an increase in the level of ALP transcripts suggests ordered deposition of mineral phase within the extracellular matrix.[46] Alkaline phosphatase is responsible for the release of orthophosphates through the cleavage of polyphosphates or pyrophosphates[47,48] which function as inhibitors of apatite formation.[49] Humans and mice lacking ALP exhibit a decrease in bone biomineralization.[48] This function for ALP suggests possible reasons why ALP is important in the mineralization process. In the present study, the difference in ALP responses may suggest one reason for the differences in mineralization that were observed with the SEM and EDS data.

With the onset of mineralization other genes are expressed.[46] This is the case for IBSP expression, usually confined to later stages of osteoblast differentiation and early stages of mineral deposition.[38] The IBSP gene codes for BSP, a protein synthesized mostly in bone tissue and involved in mineralization, constituting approximately 15% of the non-collagen matrix in young bone.[50] Furthermore, BSP is capable of binding to calcium ions and hydroxyapatite and inducing cell and collagen attachment through its cell binding and collagen binding domains, respectively. For the 6mer + BSP samples, a significant up-regulation of IBSP transcript from day 3 to day 7 of cell culture (Fig. 7) was observed. This result is in good agreement with the results for ALP gene expression, suggesting active mineralization in 6mer + BSP films.

IBSP up-regulation also reflects the induction of synthesis of other extracellular proteins,[41] such as collagen type I. Type I collagen is the most abundant extracellular matrix protein in bone tissue and is involved in early stages of the mineralization, as described earlier.[51,52] Type I collagen also functions as a scaffold where non-collagenous proteins bind to act as mineral nucleators. In this way, collagen I fibers play an important role in bone formation as both a primary building block and for higher

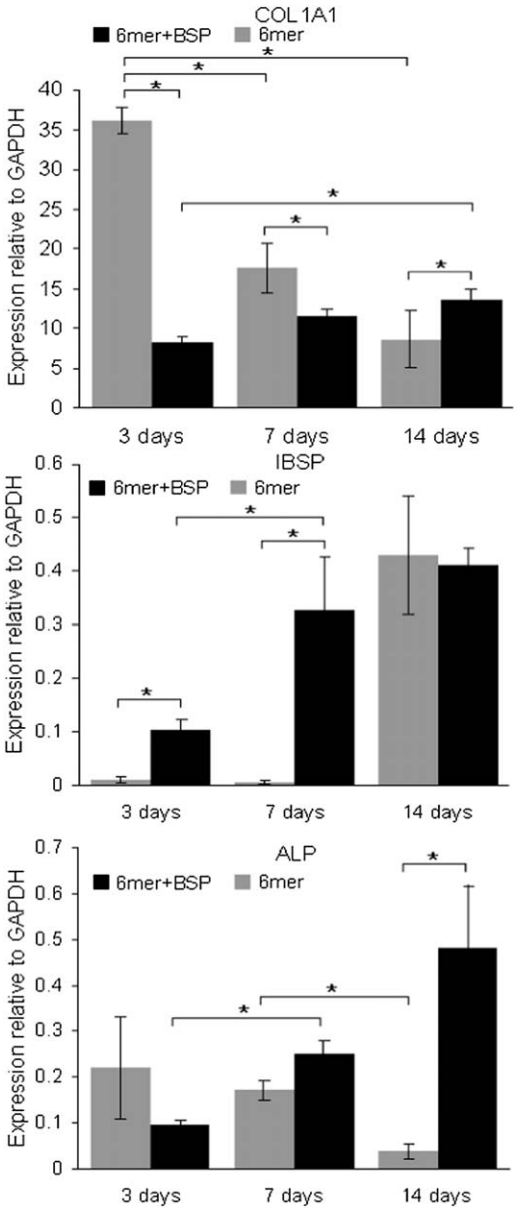

Fig. 7 Transcript levels from hMSCs cultured on the 6mer and 6mer + BSP films after 3, 7 and 14 days for genes COL1A1, ALP and IBSP. Asterisks indicate statistically significant differences ($p < 0.05$).

organized architectures related to this process.[38] The transcript data indicate significant up-regulation of COL1A1 for the 6mer + BSP samples, indicating a progressive increase of type I collagen.

In the 6mer + BSP samples, the up-regulation of COL1A1 transcripts accompanied the increase in ALP and IBSP expression levels after 3, 7 and 14 days in culture. For the 6mer samples, COL1A1 transcripts were significantly ($p < 0.05$) down-regulated between day 3 and day 14, although transcript levels were higher when compared with the 6mer + BSP samples at 3 and 7 days of cell culture. After 14 days down-regulation of COL1A1 was lower than for the 6mer + BSP samples. This significant decrease in the expression levels of COL1A1 between day 3 and day 14 of culture for 6mer samples could be due to a reduction in the metabolic activity of cells due to a reduction in cell viability as shown in Fig. 6. Also for 6mer samples the significant decrease in ALP expression levels between day 7 and day 14 and the late increase in IBSP transcripts, when compared with 6mer + BSP samples, can be indicative of a low osteogenic potential of 6mer films. Finally, the absence of COL2A1 transcript (data not shown), a marker for chondrogenic differentiation, confirmed that no chondrogenic differentiation was taking place in the 6mer + BSP or in the control 6mer samples. During culture with or without cells the protein films maintained their integrity.

Quantitative real time RT-PCR for ALP, IBSP and COL1A1 suggested that controlled mineralization was occurring on the 6mer + BSP films during culture in osteogenic medium when compared with the control 6mer films. These findings concur with the Ca/P ratios determined by EDS characterization, which increased from day 3 to 14 of culture, with an increase from 0 to 1.53–1.72, values similar to tricalcium phosphate (1.50) and hydroxyapatite (1.67), respectively.[38] The *in vitro* results suggested that the cells were actively involved in the mineralization process. Osteoblasts are the main cells responsible for the osteogenic process, involved in the deposition of bone organic matrix and in mineralization. This extracellular matrix is formed by collagen, non-collagen proteins (BSP, osteopontin, osteocalcin) and polysaccharides.[38] Osteoblasts also secrete alkaline phosphatase, an enzyme responsible for the hydrolysis of pyrophosphate, a known inhibitor of mineralization, into orthophosphate for incorporation along with calcium ions into the growing mineral lattice.[47,48,53] The osteogenic potential of the hMSCs used in the present study was confirmed by the deposition of a calcified matrix, based on both SEM and EDS analyses, as well as the real-time RT-PCR data.

Over the past decades several protein systems were described for different applications such as the development of new protein-based materials for biomedical applications.[54] Additionally, the design of new hybrid proteins, such as the ones described in the present work, may provide a new generation of high performance structures for bone regeneration applications. Recently, the recombinant spider silk protein 4RepCT was used to fabricate films, foams and fibers and *in vitro* cell viability tests showed that these mesh matrices were capable of sustained cell culture.[55] Other studies described the development of fibers through the electrospinning of recombinant spider silk MaSpI[56] and ADF-3[57] analogues, stable hydrogels fabricated from recombinant ADF-4 dragline protein with superior mechanical properties[58] and microcapsules of recombinant ADF-4 protein with high mechanical stability and suitable for drug delivery.[59] These studies highlight the versatility of silk proteins to be processed into different types of matrices according to the specific application. Furthermore, the functionalization of these silk-based materials with biologically active domains is an important strategy to influence tissue and cell responses, as is the case of the new 6mer + BSP protein described in the present study. In this study 6mer and 6mer + BSP protein films were used in the different tests. However, since this work is considered a first step towards the development of high-performance protein-based materials, other processing approaches will be used in future work for the design of more complex structures for future tissue engineering and biomedical purposes.

3. Experimental

Cloning of BSP into pET30L vector containing the silk modules

The vector pET30a+ (Novagen, San Diego CA) was used for the construction of the vector pET30L carrying the silk block copolymer and its assembly was described in our prior studies.[35] The spider silk block copolymer was cloned together with six histidine residues to facilitate purification.[35] The clone containing the bacterial plasmid pENTR223.1 carrying the human BSP cDNA sequence (Clone Identification: HsCD00082642) was purchased from the Harvard clone collection "The ORFeome Collaboration" (Dana-Farber/Harvard Cancer Center, Boston MA). The clones with pENTR223.1 plasmid carrying the BSP cDNA sequence were inoculated in Luria Bertani (LB) medium and grown overnight at 37 °C with shaking (200 rpm min^{-1}). The pENTR223.1 plasmid was extracted using a Qiagen miniprep kit (28704, Valencia, CA, USA) for plasmid isolation and digested with *Sfi*I enzyme (R0123S, New England Biolabs, Ipswich, MA, USA) which cuts in the regions flanking the BSP cDNA sequence. The digestion product was run in a 0.8% agarose gel and the band for the BSP cDNA sequence (951 bp) was purified using a QIAquick gel extraction kit (28706, Qiagen). For ligation of the BSP cDNA sequence to the 6mer spider silk clone, a linker was designed containing in its central region a restriction site for *Sfi*I for insertion of the BSP clone, and also restriction sites for *Spe*I (R0133S, New England Biolabs) and *Nhe*I (R0131S, New England Biolabs) related to the spider silk clone. For insertion of the linker in the expression vector pET30L, the vector was digested with *Spe*I, dephosphorylated with Alkaline Phosphatase, Calf Intestinal (CIP) enzyme (M0290S, New England Biolabs) and run on a 0.8% agarose gel. The linearized vector was purified using the QIAquick gel extraction kit. The linker was double digested with *Spe*I and *Nhe*I restriction enzymes generating compatible ends with those generated by *Spe*I with the expression vector pET30L. The linker was run on a 0.8% agarose gel and purified using the QIAquick gel extraction kit. The linker was then inserted in the linearized vector pET30L. The ligation reaction was carried out with T4 DNA ligase enzyme (M0202S, New England Biolabs).

Escherichia coli DH5α cells (18258-012, Invitrogen, Carlsbad, CA, USA) were transformed with the ligation product and transformants were identified by incubation on agar plates containing 25 μg ml^{-1} kanamycin. The presence of the linker in the pET30L vector was confirmed by DNA sequencing. For the insertion of the BSP cDNA sequence both vector pET30L carrying the linker (vector pET30L + linker) and vector pENTR223.1 alone were digested with *Sfi*I. In the case of the linearized vector pET30L + linker the ends generated by the digestion with *Sfi*I were dephosphorylated with CIP. After running both digestion products in a 0.8% agarose gel the bands corresponding to the BSP cDNA sequence and to the linearized vector pET30L + linker were purified using the QIAquick gel extraction kit. The ligation reaction between the vector pET30L + linker and the BSP cDNA sequence was carried out with T4 DNA ligase. *E. coli* DH5α cells transformed with the ligation product were identified by incubation in agar plates containing 25 μg ml^{-1} kanamycin. The presence of the BSP insert was confirmed by DNA sequencing (Tufts Core Facility, Boston, MA) and the new constructs were named 6mer + BSP.

Protein expression, purification and identification

Both 6mer and 6mer + BSP proteins were expressed in *E. coli* RY-3041 strain, a mutant strain of *E. coli* BLR(DE3) defective in the expression of SlyD protein.[60,61] Cells were cultivated at 37 °C in LB medium, with 25 μg ml^{-1} kanamycin until an OD_{600} between 0.9 and 1 was reached. At this point expression was induced by adding isopropyl β-D-thiogalactoside (IPTG, 15529019, Invitrogen) to a final concentration of 0.5 mM. After 2 hours cells were harvested by centrifugation at 6500 rpm. The cells pellet was resuspended in a denaturating buffer (100 mM NaH_2PO_4, 10 mM Tris–HCl, 8 M urea, pH 8.0) and left overnight with stirring for complete cell lysis. Insoluble cell fragments and soluble proteins present in the cell lysate were separated by centrifugation at 11 000 rpm. The supernatant was mixed with Ni-NTA resin (30250, Qiagen) and left for 2 hours with stirring. The supernatant/Ni-NTA resin mixture was loaded onto a glass Econo-column (Biorad, Hercules, CA, USA) and washed several times with denaturating buffer at pH 8 and at pH 6.0. The protein 6mer + BSP was eluted using denaturating buffer at pH 4.5. The purified protein was dialysed first against a 20 mM sodium acetate buffer followed by extensive dialysis against water using cellulose ester snake skin membranes with a 100–500 Da molecular weight cut off (131054, Spectra/Por Biotech, Rancho Dominguez, CA, USA). Finally, the dialyzed proteins were lyophilized.

Protein sequencing (Tufts Core Facility, Boston, MA) and SDS-PAGE were used to confirm the protein identity. For SDS-PAGE, proteins were mixed with NuPAGE LDS sample buffer (Invitrogen, NP0007) and heated at 80 °C for 10 minutes. Afterwards, the samples were separated using a bis-tris 4–12% gel (Invitrogen, NP0321BOX). For band detection was used the colloidal blue staining kit (Invitrogen, LC6025).

Film formation and secondary structure analysis

Both recombinant 6mer + BSP and 6mer proteins were dissolved in MQ water to a final concentration of 2% (w/v). Then 60 μl of each protein solution was cast into a plastic non-adherent polystyrene surface, for easier film removal, and left to dry at room temperature. The films were treated with a solution of 70% methanol in MQ water for 2 hours to induce the transition of secondary structure from random coil to β-sheet. For cell and mineralization studies the films were treated with 70% (v/v) ethanol solution for sterilization purposes.

The transition of the silk secondary structure was confirmed by ATR-FTIR (Jasco model FT/IR-6200 type A, Easton, MD, USA). Spectra were collected in absorption mode at 8 cm^{-1} resolution using 64 scans in the spectral range 4000 to 400 cm^{-1}. The quantification of secondary structure was based on the analysis of the amide I region (1700 to 1600 cm^{-1}) and 3 replicates were performed for each 6mer and 6mer + BSP protein group. The average percentage for the secondary structures, mainly β-sheet content, for the 6mer (control) and 6mer + BSP proteins were calculated through the integration of the area of each deconvoluted curve followed by the normalization of the obtained value to the total area of the amide I region.

In vitro mineralization

To investigate the mineralization potential of the new chimeric protein 6mer + BSP, a protein solution was prepared as described previously and 60 μl of this solution was used to prepare films. The films were treated with methanol as described above, and a similar procedure was carried out for the control 6mer protein. Both protein films were incubated for 1 and 6 hours at 37 °C, with an accelerated calcification solution (ACS) of 150 mM Na^+, 20 mM of HEPES, 3.75 mM Ca^{2+} and 2.32 mM PO_4^{3-}, pH 7.4.[62] At the end of the incubation periods of 1 and 6 hours the films were washed with MQ water and dried at room temperature.

In vitro hMSCs responses to 6mer and 6mer + BSP films

Human mesenchymal stem cells (hMSC) were aspirated from bone marrow originated from a young healthy donor obtained from Lonza (Walkersville, MD, USA). Frozen passage 3 hMSC stocks were thawed and seeded at 3.0×10^3 cells cm^{-2} in a 96 wells plate, containing 6mer and 6mer + BSP films, using basal medium consisting of Dulbecco's modified Eagle's medium (DMEM) supplemented with 10% (v/v) fetal bovine serum (FBS), 1% penicillin–streptomycin (v/v) and 10 ng of basic fibroblast growth factor (bFGF) at 37 °C with 5% CO_2 in a humidified environment. After cells reach 80–90% confluence culture medium was changed from basal medium to osteogenic medium consisting of in DMEM supplemented with 10% (v/v) FBS, 1% antibiotic/antimycotic, 100 nM dexamethasone, 10 mM β-glycerol phosphate and 0.05 mM ascorbic acid. Samples were collected after 3, 7 and 14 days of culture. Medium was changed every two days.

Analytical methods

Cell morphology was accessed through field-emission scanning electron microscopy (SEM) (NanoSEM, FEI Nova 200). Samples were fixed with a 2.5% glutaraldehyde solution in phosphate buffer (PBS) (v/v) and dehydrated in a series of ethanol–water solutions with increasing ethanol concentration (v/v): 25%, 30%, 50%, 70%, 80%, 90% and 100%. For SEM observation the samples were sputter coated with gold–palladium.

Alamar Blue (Invitrogen, DAL1025) assay was used to determine cell viability/proliferation after 3, 7 and 14 days of culture and 5 replicates were performed for 6mer and 6mer + BSP films for each time period. The Alamar Blue system incorporates an oxidation–reduction indicator (redox indicator) that fluoresces and changes colour as a result of chemical reduction of growth media due to cell metabolic activity. This redox indicator was demonstrated to be minimally toxic to cells. Alamar Blue reagent was added to the growth media in a 1 : 10 dilution ratio and data were collected using fluorescence at a 530–560 nm excitation wavelength and 590 nm emission wavelength.[63]

For quantitative real time reverse transcription-polymerase chain reaction (real time RT-PCR) the mRNA of cells was extracted using RNeasy mini kits (Qiagen, 74106) and cDNA synthesis was performed using a High Capacity cDNA Reverse Transcription Kit (Applied Biosystems, 4368814). For the PCR reaction the TaqMan Universal PCR Master Mix (Applied Biosystems, 4304437) was used, following the procedure provided by the supplier, and the Taqman Gene Expression Assay was used to access the expression of the following genes: COL1A1 (collagen type I alpha 1, Hs00164004_m1), IBSP (integrin bone sialoprotein, Hs00173720_m1), ALP (alkaline phosphatase, Hs00758162_m1), GAPDH (Glyceraldehyde 3-phosphate dehydrogenase, Hs99999905_m1) and COL2A1 (collagen type II alpha 2, Hs01064869_m1). Results were normalized to GAPDH expression used as a housekeeping marker. 9 replicates were performed for each gene.

6mer and 6mer + BSP film characterization

Surface morphology of 6mer + BSP and 6mer films before and after incubation in ACS for different periods of time was characterized using field-emission scanning electron microscopy (SEM) (NanoSEM, FEI Nova 200). Samples were sputter coated with gold–palladium for SEM observation. Elemental composition of the mineral deposited on the surface of the protein films was characterized by an energy dispersive spectrometer (EDS) (EDAX- Pegasus X4M) and no coating was used for this analysis. SEM and EDS characterizations were also used to characterize 6mer + BSP and 6mer films after 3, 7 and 14 days of cell culture in osteogenic medium to access mineral deposition. 6mer + BSP and 6mer films cultured only with osteogenic medium, with no cells, were used as controls to test for the possible influence of cells on mineral deposition. For SEM, samples were sputter coated with gold–palladium and as mentioned before no coating was used for EDS analysis. At least 3 replicates were used in each analysis.

Statistical analysis

SPSS 17.0 was used to perform statistical analysis. The Shapiro–Wilk test was used to test for the normality of the data. To compare between two sets of data mainly 6mer + BSP *vs.* 6mer films (control) two statistical tests were used: two-tailed nonparametric Mann–Whitney test for non-normal distributed data and Student *t*-test to analyse data with normal distributions. To test for significant differences between three experimental groups (3, 7 and 14 days) one-way ANOVA with a Bonferroni post hoc comparison was applied to the data with normal distribution and nonparametric Kruskal–Wallis test was used for the data with non-normal distribution. Statistical significance was defined as $p < 0.05$.

4. Conclusions

In summary, the successful design of a new chimeric protein conjugating spider silk with human bone sialoprotein (BSP) is described. The combination of both silk and BSP domains in a single protein chain did not interfere with the functions of each of the domains. This includes the ability of the spider silk to self-organize into a β-sheet conformation, an important feature related with its mechanical properties, and the aptitude of BSP to induce the nucleation of calcium phosphates. During the 14 days of culture this new chimeric protein sustained hMSC proliferation and differentiation into the osteogenic lineage. These data are evident for cells seeded onto the 6mer + BSP, indicating that the conjugation with the amino acid sequence of human BSP

improves cellular function towards the osteoblastic phenotype. These promising results suggest the potential for this chimeric protein as a new biomaterial for tissue engineering applications, especially for the construction of grafts for bone regeneration. Additionally, these results also highlight the potential of chimeric proteins as multifunctional biomaterial systems allowing the control over different types of cellular response such as cell differentiation, cell migration and cell adhesion, and protein adsorption, among others. The importance of this approach relies on the ability to bioengineer nanoscale composite systems that can be used in the fabrication of new families of biomaterials capable of self-modification either before, *in vitro*, or after implantation, *in vivo*.

Acknowledgements

The authors acknowledge Olena Rabotyagova for advice in protein sequence design. Sílvia Gomes thanks Portuguese Foundation for Science and Technology (FCT) for providing her PhD grant SFRH/BD/28603/2006. This work was carried out under the scope of European NoE EXPERTISSUES (NMP3-CT-2004-500283), the FIND & BIND project funded by the agency EU-EC (FP7 program), the FCT R&D project Proteo-Light (PTDC/FIS/68517/2006) funded by the FCT agency, the Chimera project (PTDC/EBB-EBI/109093/2008) funded by the FCT agency, and the NIH (P41 EB002520) Tissue Engineering Resource Center and the NIH (EB003210 and DE017207).

Notes and references

1 M. Kruyt, D. Delawi, P. Habibovic, F. Oner, C. v. Blitterswijk and W. Dhert, *J. Orthop. Res.*, 2009, **27**, 1055–1059.
2 J. Dawson and R. Oreffo, *Arch. Biochem. Biophys.*, 2008, **473**, 124–131.
3 P. C. Bessa, E. R. Balmayor, H. S. Azevedo, S. Nürnberger, M. Casal, M. v. Griensven, R. L. Reis and H. Redl, *J. Tissue Eng. Regener. Med.*, 2010, **4**, 349–355.
4 C. A. Custódio, C. M. Alves, R. L. Reis and J. F. Mano, *J. Tissue Eng. Regener. Med.*, 2010, **4**, 316–323.
5 J. F. Mano and R. L. Reis, *J. Tissue Eng. Regener. Med.*, 2007, **4**, 261–273.
6 M. Xu and R. V. Lewis, *Proc. Natl. Acad. Sci. U. S. A.*, 1990, **87**, 7120–7124.
7 T. Scheibel, *Microb. Cell Fact.*, 2004, **3**, 14–24.
8 C. Hayashi, N. Shipley and R. Lewis, *Int. J. Biol. Macromol.*, 1999, **24**, 271–275.
9 J. D. v. Beek, S. Hess, F. Vollrath and B. H. Meier, *Proc. Natl. Acad. Sci. U. S. A.*, 2002, **99**, 10266–10271.
10 E. Bini, C. W. P. Foo, J. Huang, V. Karageorgiou, B. Kitchel and D. L. Kaplan, *Biomacromolecules*, 2006, **7**, 3139–3145.
11 O. Rabotyagova, P. Cebe and D. L. Kaplan, *Biomacromolecules*, 2009, **10**, 229–236.
12 G. H. Altman, F. Diaz, C. Jakuba, T. Calabro, R. L. Horan, J. Chen, H. Lu, J. Richmond and D. L. Kaplan, *Biomaterials*, 2003, **24**, 401–416.
13 C. W. P. Foo, S. Patwardhan, D. Belton, B. Kitchel, D. Anastasiades, J. Huang, R. Naik, C. Perry and D. Kaplan, *Proc. Natl. Acad. Sci. U. S. A.*, 2006, **103**, 9428–9433.
14 J. Huanga, C. Wonga, A. Georgeb and D. L. Kaplan, *Biomaterials*, 2007, **28**, 2358–2367.
15 A. Bellahcène, K. Bonjean, B. Fohr, N. S. Fedarko, F. A. Robey, M. F. Young, L. W. Fisher and V. Castronovo, *Circ. Res.*, 2000, **86**, 885–891.
16 M. Mizuno, T. Imai, R. Fujisawa, H. Tani and Y. Kuboki, *Calcif. Tissue Int.*, 2000, **66**, 388–396.
17 P. Valverde, J. Zhang, A. Fix, J. Zhu, W. Ma, Q. Tu and J. Chen, *J. Bone Miner. Res.*, 2008, **23**, 1775–1778.
18 A. Karadag, K. Ogbureke, N. Fedarko and L. Fisher, *J. Natl. Cancer Inst.*, 2004, **96**, 956–965.
19 A. Karadag and L. Fisher, *J. Bone Miner. Res.*, 2006, **21**, 1627–1636.
20 B. Rapuano, C. Wu and D. MacDonald, *J. Orthop. Res.*, 2004, **22**, 353–361.
21 M. T. Bernards, C. Qin and S. Jiang, *Colloids Surf., B*, 2007, **64**, 236–247.
22 M. T. Bernards, C. Qin, B. D. Ratner and S. Jiang, *J. Biomed. Mater. Res., Part A*, 2007, 779–787.
23 L. Xu, A. Anderson, Q. Lu and J. Wang, *Biomaterials*, 2007, **28**, 750–761.
24 J. Wang, H. Zhou, E. Salih, L. Xu, L. Wunderlich, X. Gu, J. Hofstaetter, M. Torres and M. Glimcher, *Calcif. Tissue Int.*, 2006, **79**, 179–189.
25 H. Graf, S. Stoeva, F. Armbruster, J. Neuhaus and H. Hilbig, *Int. J. Oral Maxillofacial Surg.*, 2008, **37**, 634–640.
26 G. Baht, G. Hunter and H. Goldberg, *Matrix Biol.*, 2008, **27**, 600–608.
27 R. Fujisawa, Y. Nodasaka and Y. Kuboki, *Calcif. Tissue Int.*, 1995, **56**, 140–144.
28 L. Fisher, D. Torchia, B. Fohr, M. Young and N. Fedarko, *Biochem. Biophys. Res. Commun.*, 2001, **280**, 460–465.
29 H. Goldberg, K. Warner, M. Li and G. Hunter, *Connect. Tissue Res.*, 2001, **42**, 25–37.
30 N. Fedarko, B. Fohr, P. Robey, M. Young and L. Fisher, *J. Biol. Chem.*, 2000, **275**, 16666–16672.
31 S. Arcidiacono, C. Mello, D. Kaplan, S. Cheley and H. Bayley, *Appl. Microbiol. Biotechnol.*, 1998, **49**, 31–38.
32 J. M. Smeenk, P. Schön, M. B. J. Otten, S. Speller, H. G. Stunnenberg and J. C. M. v. Hest, *Macromolecules*, 2006, **39**, 2989–2997.
33 M. W. T. Werten, A. P. H. A. Moers, T. Vong, H. Zuilhof, J. C. M. v. Hest and F. A. d. Wolf, *Biomacromolecules*, 2008, **9**, 1705–1711.
34 W. B. Jeon, *BMB Rep.*, 2011, **44**, 22–27.
35 O. Rabotyagova, P. Cebe and D. Kaplan, *Biomacromolecules*, 2009, **10**, 229–236.
36 C. W. P. Foo, E. Bini, J. Huang, S. Y. Lee and D. L. Kaplan, *Appl. Phys. A: Mater. Sci. Process.*, 2006, **82**, 193–203.
37 O. Rabotyagova, P. Cebe and D. Kaplan, *Macromol. Biosci.*, 2010, **10**, 49–59.
38 L. Palmer, C. Newcomb, S. Kaltz, E. Spoerke and S. Stupp, *Chem. Rev.*, 2008, **108**, 4754–4783.
39 C. Schmidt, D. Kaspar, M. Sarkar, L. Claes and A. Ignatius, *J. Biomed. Mater. Res.*, 2002, **63**, 252–261.
40 B. Ananthanarayanan, L. Little, D. V. Schaffer, K. E. Healy and M. Tirrell, *Biomaterials*, 2010, **31**, 8706–8715.
41 A. Higuchi, Y. Takanashi, N. Tsuzuki, T. Asakura, C.-S. Cho, T. Akaike and M. Hara, *J. Biomed. Mater. Res.*, 2003, **65**, 369–378.
42 J. Chen, G. H. Altman, V. Karageorgiou, R. Horan, A. Collette, V. Volloch, T. Colabro and D. L. Kaplan, *J. Biomed. Mater. Res.*, 2003, **67**, 559–570.
43 E. S. Gil, B. B. Mandal, S.-H. Park, J. K. Marchant, F. G. Omenetto and D. L. Kaplan, *Biomaterials*, 2010, **31**, 8953–8963.
44 S. Sofia, M. B. McCarthy, G. Gronowicz and D. L. Kaplan, *J. Biomed. Mater. Res.*, 2001, **54**, 139–148.
45 P. Choong, T. J. Martin and K. W. Ng, *J. Orthop. Res.*, 1993, **11**, 638–647.
46 J. Lian and G. Stein, *Iowa Orthop. J.*, 1995, **15**, 118–140.
47 A. Hirschler, J. Lucas and J. Hubert, *FEMS Microbiol. Lett.*, 1990, **73**, 211–220.
48 M. Murshed, D. Harmey, J. Millán, M. McKee and G. Karsenty, *Genes Dev.*, 2005, **19**, 1093–1104.
49 H. Fleish and W. Neuman, *Am. J. Physiol.*, 1961, **200**, 1296–1300.
50 L. Meinel, V. Karageorgiou, S. Hofmann, R. Fajardo, B. Snyder, C. Li, L. Zichner, R. Langer, G. Vunjak-Novakovic and D. L. Kaplan, *J. Biomed. Mater. Res.*, 2004, **71A**, 25–34.
51 S. Jackson, *Proc. R. Soc. London, Ser. B*, 1956, **146**, 270–280.
52 S. Weiner and H. Wagner, *Annu. Rev. Mater. Sci.*, 1998, **28**, 271–298.
53 M. Balcerzak, E. Hamade, L. Zhang, S. Pikula, G. Azzar, J. Radisson, J. Bandorowicz-Pikula and R. Buchet, *Acta Biochim. Pol.*, 2003, **50**, 1019–1038.
54 M. Yang, C. Tanaka, K. Yamauchi, K. Ohgo, M. Kurokawa and T. Asakura, *J. Biomed. Mater. Res., Part A*, 2008, **84**, 353–363.
55 M. Widhe, H. Bysell, S. Nystedt, I. Schenning, M. Malmsten, J. Johansson, A. Rising and M. Hedhammar, *Biomaterials*, 2010, **31**, 9575–9585.

56 S. Arcidiacono, C. M. Mello, M. Butler, E. Welsh, J. W. Soares, A. Allen, D. Ziegler, T. Laue and S. Chase, *Macromolecules*, 2002, **35**, 1262–1266.
57 A. Lazaris, S. Arcidiacono, Y. Huang, J.-F. Zhou, F. Duguay, N. Chretien, E. A. Welsh, J. W. Soares and C. N. Karatzas, *Science*, 2002, **295**, 472–476.
58 S. Rammensee, D. Huemmerich, K. D. Hermanson, T. Scheibel and A. R. Bausch, *Appl. Phys. A: Mater. Sci. Process.*, 2006, **82**, 261–264.
59 K. D. Hermanson, D. Huemmerich, T. Scheibel and A. R. Bausch, *Adv. Mater.*, 2007, **19**, 1810–1815.
60 S. Z. Yan, J. A. Beeler, Y. Chen, R. K. Shelton and W. J. Tang, *J. Biol. Chem.*, 2001, **276**, 8500–8506.
61 J. Huang, R. Valluzzi, E. Bini, B. Vernaglia and D. L. Kaplan, *J. Biol. Chem.*, 2003, **278**, 46117–46123.
62 Q. Liu, J. Weng, J. Wijn and T. Blitterswijk, *Fifth World Biomaterials Congress*, Toronto, 1996.
63 M. Lancaster, and R. Fields, *USPat.*, 5 501 959, 1996.